

A novel telomere-related gene prognostic signature for survival and drug treatment efficiency prediction in lung adenocarcinoma

Haiming Chen^{1,*}, Weiwan Liang^{2,*}, Weiqiang Zheng^{2,*}, Feilong Li¹, Xingxi Pan¹, Yiyu Lu¹

¹Department of Oncology, The Sixth Affiliated Hospital, School of Medicine, South China University of Technology, Foshan, Guangdong Province 528200, China

²Department of Respiration, Foshan Second People's Hospital, Foshan, Guangdong Province 528000, China

*Equal contribution and shared co-first authorship

Correspondence to: Yiyu Lu, Xingxi Pan; **email:** lyuyiyi@scut.edu.cn, lypanxx@scut.edu.cn

Keywords: telomere, telomere-related gene, prognosis, lung adenocarcinoma

Received: April 17, 2023

Accepted: June 19, 2023

Published: August 16, 2023

Copyright: © 2023 Chen et al. This is an open access article distributed under the terms of the [Creative Commons Attribution License](https://creativecommons.org/licenses/by/3.0/) (CC BY 3.0), which permits unrestricted use, distribution, and reproduction in any medium, provided the original author and source are credited.

ABSTRACT

Objective: Telomere-related genes (TRGs) play a critical role in various types of tumors. However, there is a lack of comprehensive exploration of their relevance in lung cancer. This research aimed to verify the relationship between TRGs gene expression and the prognosis of patients with lung adenocarcinoma (LUAD), as well as the prediction of drug treatment efficiency.

Methods: A total of 2093 TRGs were acquired from TelNet. The clinical information including age, tumor stage, follow up and outcome (death/survival) and TRGs expression profile of LUAD were obtained from the patients in The Cancer Genome Atlas (TCGA) database and the Clinical Proteomic Tumor Analysis Consortium (CPTAC) database. The two databases were used to construct and verify a prognostic model based on the expression of hubTRGs. The tumor mutation burden, immune infiltration and subtypes, as well as IC50 prediction of multiple targeted drugs were also evaluated in TRGs-divided risk groups.

Results: A total of 335 TRGs were significantly differentially expressed in LUAD as compared with normal control. Among them, 9 TRGs (ABCC2, ABCC8, ALDH2, FOXP3, GNMT, JSRP1, MACF1, PLCD3, SULT4A1) were finally identified as hubGenes and used to construct a TRG risk score. The TRG risk score showed favorable performance in constructing a prognostic nomogram in predicting survival of LUAD, and the ROC curves at 1, 3 and 5 years were plotted and the AUROC values were 0.743, 0.754 and 0.735, respectively. Higher TRGs risk score correlated with worse immune subtypes and higher tumor mutation burden in LUAD tissues. In addition, the patients in TRG high risk group harbored a lower TIDE score which indicated potentially better response to immunotherapy.

Conclusion: This study proposed a broad molecular signature of telomere-related genes that can be used in further functional and therapeutic investigations, and also represents an integrated modality for characterizing critical molecules when exploring novel targets for lung cancer immunotherapy.

INTRODUCTION

Lung cancer is the most common type of cancer worldwide, and lung adenocarcinoma (LUAD) is a major histologic subtype of lung cancer [1, 2]. The classic prognostic factors of LUAD are usually demographic factors such as age, complication and

tumor-related parameters including tumor stage, node stage and metastasis stage [3, 4]. In recent years, due to the progress of sequencing technology, some models based on genetic signatures have been explored to evaluate the prognosis of LUAD patients. These models have shown a promising predictive accuracy, and a few of them might also

indicate the potential carcinogenesis mechanism of LUAD [5–7].

Telomeres are important regions at the end of chromosomes and composed of repetitive TTAGGG DNA sequences and shelterin complex [8]. In normal lung tissues, telomeres are vital for chromosome integrity, cellular replication and protection against activation of DNA damage response [9]. Telomere attrition results in cell cycle arrest and might be followed by cell division and certain disease status. Disorder of telomeres can lead to various diseases such as cardiac disease, dyskeratosis congenita and cancers [10]. Telomere length maintenance is crucial for the limitless proliferation of human cancer cells owing to the 3'-end erosion, a process intrinsic to the replication of linear chromosomes. Continual telomere shortening keeps somatic cells from aberrant proliferation and tumorigenesis by induction of senescence or apoptosis [11]. Research has reported that cancer cells with proliferative function can solve the problem of telomere shortening through a functional ribonuclease protease complex, namely telomerase [12]. The change in telomere length is related to the risk of lung cancer and may serve as a prognostic indicator for lung cancer patients [13]. However, cancer cells can circumvent this restriction by possessing a telomere maintenance mechanism (TMM) [14].

Recently, emerging studies have implied that TMM in cancer is a complicated process that is associated with hundreds of various genes [15]. These telomere-related genes (TRGs) have also shown significant relevance to the prognosis of several types of cancer. In kidney renal clear cell cancer, a risk score developed by using the expression level of TRGs is correlated with immune subtypes and tumor mutation burden, as well as can predict the outcomes of kidney cancer patients [16]. In the study by Liu et al., an 18-telomere length-related gene prognostic signature is developed in non-small cell lung cancer to assess tumor immunity and predict response to PDL-1 blockade immune therapy [17]. However, they only used 168 TRGs in the analysis while the total number of TRGs that are reported to be involved in telomere maintenance has exceeded 2000 [18]. Thus, a more comprehensive analysis is needed to further understand the signature of TRGs in lung cancer.

Herein, we aim to exhaustively explore the distinct features of TRGs in LUAD. Based on the TRGs, we constructed a risk model to predict the prognosis of LUAD and then investigate the potential role of this risk model in selecting treatment agents. This study represents the systematic investigation of telomere-related molecular signatures in LUAD, which offers a

deeper genetic understanding of this cancer and facilitates the development of LUAD subtype-specific therapeutic strategy.

METHODS

Databases and online analytical tools used in this study

The transcriptome profiling data and survival information of patients with LUAD in the training set were downloaded from The Cancer Genome Atlas (TCGA) database (TCGA-LUAD project) via the Genomic Data Commons (GDC) data portal. The tumor mutation burden (TMB) information of the TCGA-LUAD cohort were also obtained. The data of patients with LUAD in the validation set were acquired from Clinical Proteomic Tumor Analysis Consortium (CPTAC) database (CPTAC-3 project) via the GDC data portal. The protein expression level in LUAD were explored in CPTAC database and the immunohistochemical (IHC) staining image of LUAD were identified in the Human Protein Atlas (HPA) database. The estimation of immune cells infiltration in the LUAD tumor microenvironment was evaluated by selected genes analysis using CIBERSORTx [19]. The gene list of TRGs were obtained from TelNet database which offers a comprehensive compilation of more than 2000 human genes linked to telomere maintenance [18].

Analysis of differentially expressed TRGs in TCGA-LUAD cohort

The downloaded expression profile of TCGA-LUAD were processed via normalization by the DESeq2 package in R (version 4.2.2). Principal component analysis (PCA) was performed to compare the expression profile between tumor and normal tissues. The differentially expressed TRGs between tumor and normal tissues were analysed by using the DESeq2 package in R (version 4.2.2). Differentially expressed TRGs were defined as genes with the logFC (fold change) of expression >1 or <-1 and adjusted P value < 0.01 . The volcano plot and heatmap were illustrated to present these differentially expressed TRGs by using the ggplot2 package and pheatmap package in R (version 4.2.2), respectively.

Identification of HubTRGs in the survival of LUAD patients and calculation of TRG risk score

To screen the TRGs that had significant relationship with LUAD prognosis, univariate analysis was performed by using Kaplan-Meier (K-M) method and univariate COX regression method. The Kaplan-Meier method compared the high-expression and low-

expression of TRGs as dichotomous variables while univariate COX regression method evaluated TRGs as continuous variable. The TRGs that were overlapped in the significant genes identified by the two methods were used for further Lass regression and multivariate COX regression. The stepwise procedure was used to determine the final hubTRGs which were included in the risk score model. These survival analyses were performed using survival, survminer and glmnet packages in R.

Construction and verification of prognostic nomogram

A prognostic nomogram to predict the 1-, 3-, and 5-year survival rates was constructed with the variables including TRG risk score, age and AJCC pathologic stage by using rms package in R (version 4.2.2). To verify the nomogram in the training set, the calibration curve and receiver operating characteristic (ROC) curve at 1-, 3-, and 5-year was plotted to estimate the accuracy of the nomogram in predicting the prognosis by using rms, pROC and timeROC packages in R (version 4.2.2). For external validation, the same analyses were also performed in the CPTAC LUAD cohort.

TMB analysis

The tumor mutation burden was analysed in the TCGA-LUAD cohort and downloaded via the GDC data portal. The correlation between TRG risk score, expression level of hubTRGs and TMB were analysed by using the cor.test function in R (version 4.2.2). The TRG risk score, expression level of hubTRGs of each patient were divided as high level and low-level groups, and the TMB level was analysed in these groups.

Immune characteristics evaluation and immune subtype estimation

The infiltration of the 22 types of immune cells including macrophages, CD4⁺T cells, CD8⁺T cells, B cells, ect. in the LUAD tumor microenvironment was investigated by using specific genes' expression profile using CIBERSORTx. The relationship between 22 types of immune cells with TRG risk score was also investigated.

The immune subtypes of LUAD in the TCGA database was acquired by using the TCGAAbiolinks package in R (version 4.2.2). The immune subtypes were compared in the high and low TRG risk score groups. Besides, the Tumor ImmuneDysfunction and Exclusion (TIDE) score was calculated by using an online tool provided according to the instructions.

IC50 prediction of multiple targeted drugs

The half-maximal inhibitory concentrations (IC50) of targeted therapeutic agents were predicted using the gene expression level to reflect the treatment sensitivity. This was performed using the oncoPredict package in R (version 4.2.2) [20].

Statistical analysis

The analysis in this study was performed using R (version 4.2.2). The distribution normality for continuous variables was evaluated by Shapiro-Wilk test. If the continuous variables were normally distributed, they were compared by student's t-test; otherwise, Wilcoxon ranked-sum test was conducted. $P < 0.05$ (two sides) was considered as statistically significant.

Data availability

All data generated or analysed during this study are included in this article and its supplementary material files. Further enquiries can be directed to the corresponding author.

RESULTS

Differentially expressed TRGs in LUAD

A total of 2093 TRGs were acquired from TelNet. The expression of these genes was compared between TCGA-LUAD tumor tissues and normal controls. PCA plot showed discrete scatter points of the two groups (Figure 1A). Among the 2093 TRGs, 335 were significantly differentially expressed in LUAD ($|\logFC| > 1$ and adjusted P value < 0.01). Among these, 159 were up-regulated and 176 were down-regulated (Figure 1B). The detailed expression information of the 2093 TRGs were available in Supplementary Table 1 and Figure 1C.

Construction and verification of TRG risk model in predicting the prognosis of LUAD patients

As shown in Supplementary Table 2, K-M method revealed 86 TRGs that were correlated with survival and univariate COX regression revealed 108 TRGs with $P < 0.05$. Among the 108 TRGs, 51 were risk genes with $HR > 1$ and 57 were protective with $HR < 1$ (Figure 2A). There were 74 genes that were overlapped in the results of the two methods. Then 19 out of 74 genes were screened by using Lasso regression. With further stepwise selection, a total of 9 hubTRGs were finally identified (Table 1). Using multivariate COX regression analysis, the TRG risk score were calculated

with the following formula: $ABCC2 \times 0.0411 - ABCC8 \times 0.0785 - ALDH2 \times 0.1519 - FDX1 \times 0.1557 - GNMT \times 0.1039 - JSRP1 \times 0.0862 - MACF1 \times 0.214 + PLCD3 \times 0.1535 - SULT4A1 \times 0.0562$. The TRG risk score of patients in the TCGA-LUAD cohort was computed, and the patients were divided into high and low risk groups based on each patient's median TRG risk score value. The K-M curve was plotted and shown in Figure 2B. The hubTRG-high risk group had

significantly worse survival outcome as compared with low risk group (median survival: 35.8 versus 72.5 months, $P < 0.0001$). The mRNA expression and protein levels were shown in Figure 2C–2E.

As the final TRG risk model, a nomogram was constructed based on the TRG risk score, age and AJCC pathologic stage (Figure 3A). In the nomogram, the coefficient values of TRG risk score, age and AJCC

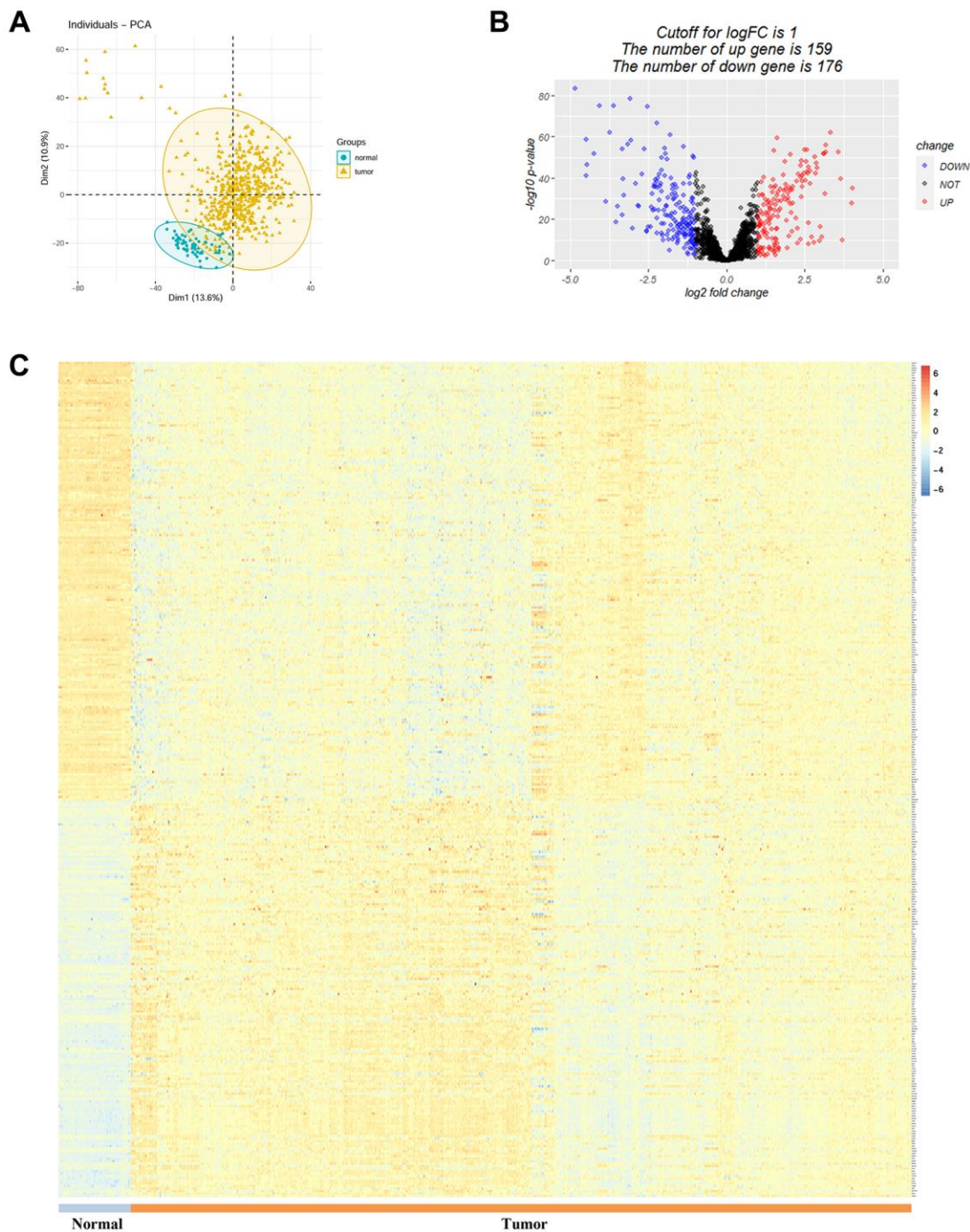


Figure 1. Analysis of differentially expressed telomere-related genes in LUAD. (A) Principal component analysis between LUAD and normal control. **(B)** and **(C)** Volcano plot and heatmap showing the up-regulated and down-regulated telomere-related genes in LUAD.

Table 1. Parameters of the TRG risk score calculation.

TRG	LogFC in LUAD	Co.ef in the multivariable COX model	Standard error of Co.ef	P value of TRG in the multivariable COX model
ABCC2	1.18	0.0411	0.028	0.142
ABCC8	-2.02	-0.0785	0.0377	0.037
ALDH2	-1.59	-0.1519	0.0742	0.041
FOXP3	1.49	-0.1557	0.0805	0.053
GNMT	-1.61	-0.1039	0.0648	0.109
JSRP1	2.09	-0.0862	0.0438	0.049
MACF1	-1.16	-0.2140	0.098	0.029
PLCD3	-1.13	0.1535	0.0669	0.022
SULT4A1	1.67	-0.0562	0.031	0.071

Abbreviations: TRG: telomere-related gene; LUAD: lung adenocarcinoma.

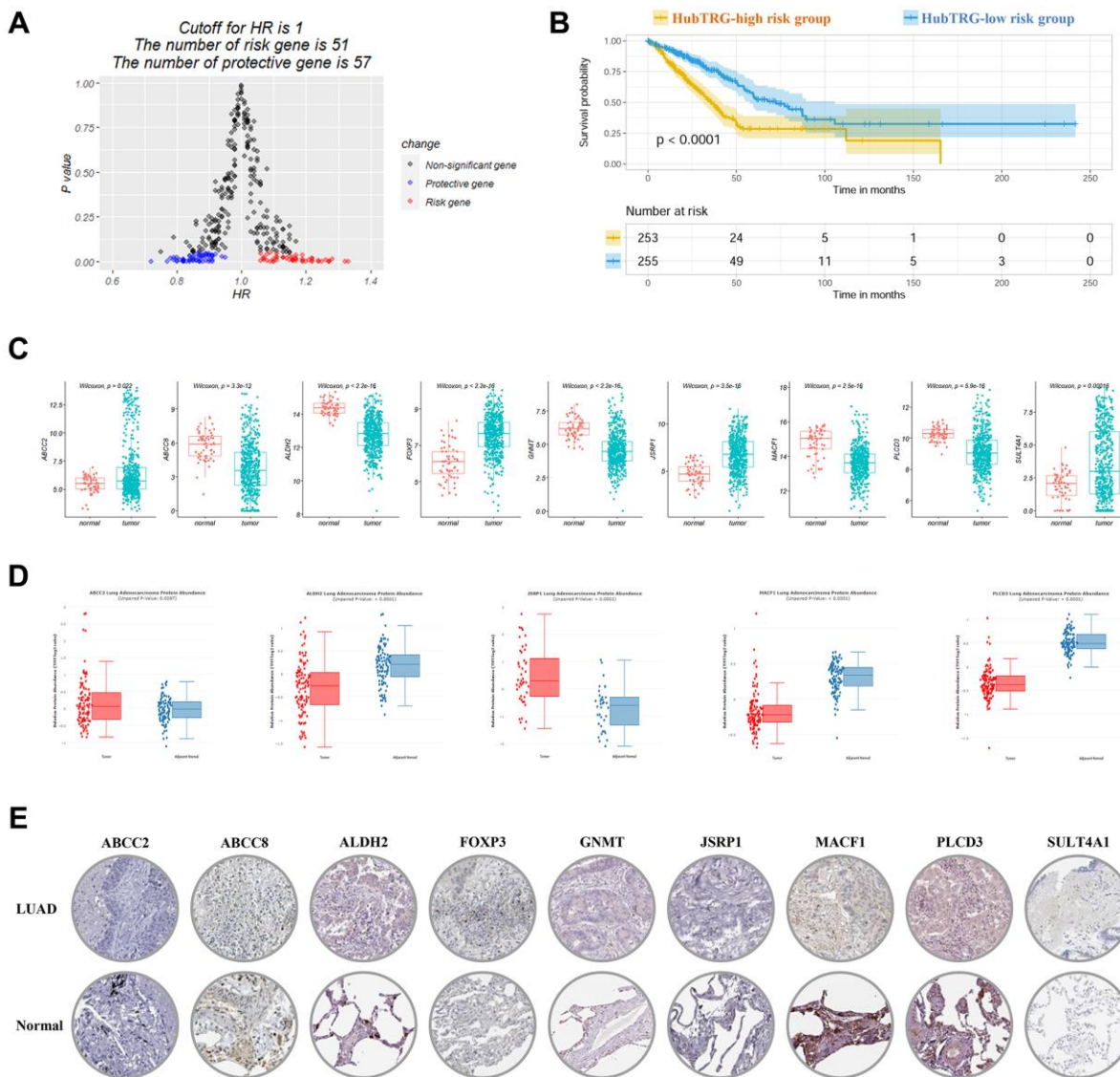


Figure 2. Risk score calculated by using nine hub-telomere-related genes (TRGs) in LUAD. (A) Volcano plot showing the significant genes and hazard ratio values in univariate COX regression analysis. **(B)** Survival curves of high and low TRG risk score groups plotted by K-M method. **(C)** Boxplots of nine hubTRGs mRNA expression in LUAD. **(D)** and **(E)** Boxplots and immunohistochemistry staining of the nine hub-telomere-related proteins in LUAD and normal control.

pathologic stage were 0.9816, 0.1828 and 0.4197, respectively. Based on the nomogram, the patients in the TCGA-LUAD cohort were divided into high and low risk groups and K-M curve revealed significantly reduced survival in high risk group (Figure 3B). The calibration curves showed good fitting of predicted survival and actual survival at 3 years and 5 years (Figure 3C). The ROC curves at 1, 3 and 5 years were plotted and the AUROC values were 0.743, 0.754 and 0.735, respectively (Figure 3D).

To further evaluate the accuracy of the nomogram, it was validated in an external CPTAC-LUAD cohort. The nomogram-divided risk groups showed significantly different survival within 60 months follow-up (Figure 4A). The calibration curves showed fitting of predicted survival and actual survival at 1 year, 3 years and 5 years (Figure 4B). The AUROC values at 1, 3 and 5 years were 0.712, 0.741 and 0.705, respectively (Figure 4C). In brief, the nomogram based on TRG risk score performed well in predicting prognosis of LUAD patients in both the training set and validation set.

Patients with high TRG risk score showed higher TMB

The TRG risk score showed a positive correlation with the TMB ($R = 0.129$, $P = 0.075$, Figure 5A). The patients in the high TRG risk score group showed a higher TMB ($P = 0.024$) than those in the low risk group (Figure 5B). The correlation of 9 hubTRGs with TMB were also presented in Figure 5.

TRG risk score indicated different immune cells infiltration status

The infiltration status of 22 types of immune cells was evaluated high and low TRG risk groups (Figure 6A). The infiltration of 14 types of immune cells were significantly correlated with TRG risk score ($P < 0.05$, Figure 6B), while 7 types of immune cells showed significant difference between high and low TRG risk groups ($P < 0.05$, Figure 6C).

In previous research, the cancers of each individual in the TCGA database have been clustered into six

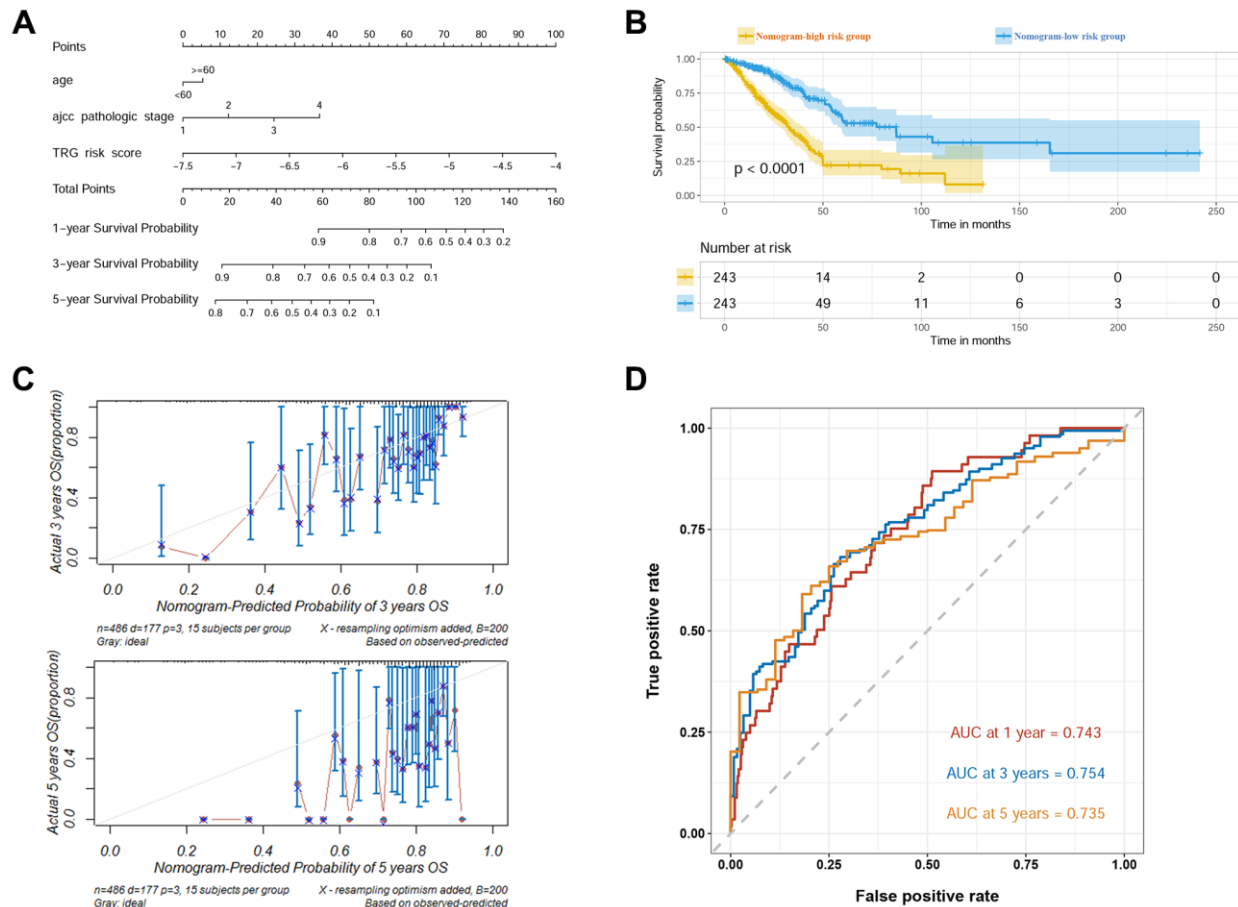


Figure 3. Construction of the prognostic nomogram in TCGA cohort. (A) Visualized nomogram based on age, AJCC stage, and TRG risk score. (B) Survival curves of high and low nomogram risk groups plotted by K-M method. (C) Calibration curves of the nomogram at 3 and 5 years. (D) ROC curves of the nomogram at 1, 3 and 5 years.

subtypes based on the immune status: C1 (wound healing), C2 (IFN-g dominant), C3 (inflammatory), C4 (lymphocyte depleted), C5 (immunologically quiet), and C6 (TGF-b dominant) [21]. We analysed the immune subtypes in high and low TRG risk groups. The results showed that high TRG risk group had a higher proportion of C3 (25%) and C6 (25%) subtypes and a lower proportion of C1 (7%), C2 (13%), C4 (13%) and C5 (17%) subtypes than the patients in the low risk group ($P = 0.005$, Figure 7A).

The TIDE score was significantly lower in the TRG high risk group than in the low-risk group ($P < 0.001$, Figure 7B). The TIDE score showed significantly negative correlation with TRG risk score ($R = -0.423$, $P < 0.001$, Figure 7C). Similarly, the exclusion score was significantly lower in the TRG high risk group than in the low-risk group ($P < 0.001$, Figure 7D). The TIDE score was significantly negative correlated with TRG risk score ($R = -0.38$, $P < 0.001$, Figure 7E).

TRG risk score in choosing treatment strategy

The top ten drugs with the least IC50 values were identified: Bortezomib, Dactinomycin, Docetaxel, Daporinad, Sepantronium bromide, Vinblastine, Eg5,

Staurosporine, Vinorelbine and Dinaciclib. Among these drugs, the IC50 values of Bortezomib, Docetaxel and Staurosporine in the high TRG risk group were significantly lower than in the low risk group, while Eg5 had a significantly higher IC50 value in the high TRG risk group (Figure 8).

DISCUSSION

TRGs play a critical role in various types of tumors. However, there is a lack of comprehensive exploration of their relevance in lung cancer [22–25], especially in LUAD. This research aimed to verify the relationship between TRGs gene expression and the prognosis of patients with LUAD, as well as the prediction of drug treatment efficiency. To the best of our understanding, this study is the first to explore the hubGenes among more than 2000 TRGs in the prognosis of LUAD. We established a prognostic nomogram based on TRGs using public databases. We found that the TRG risk score can serve as a potential tool for selecting therapeutic drugs for LUAD.

C6 (TGF- β Dominant) subtype usually account for a small group and do not dominant in major TCGA subtypes [16]. However, in this study the C6 subtype

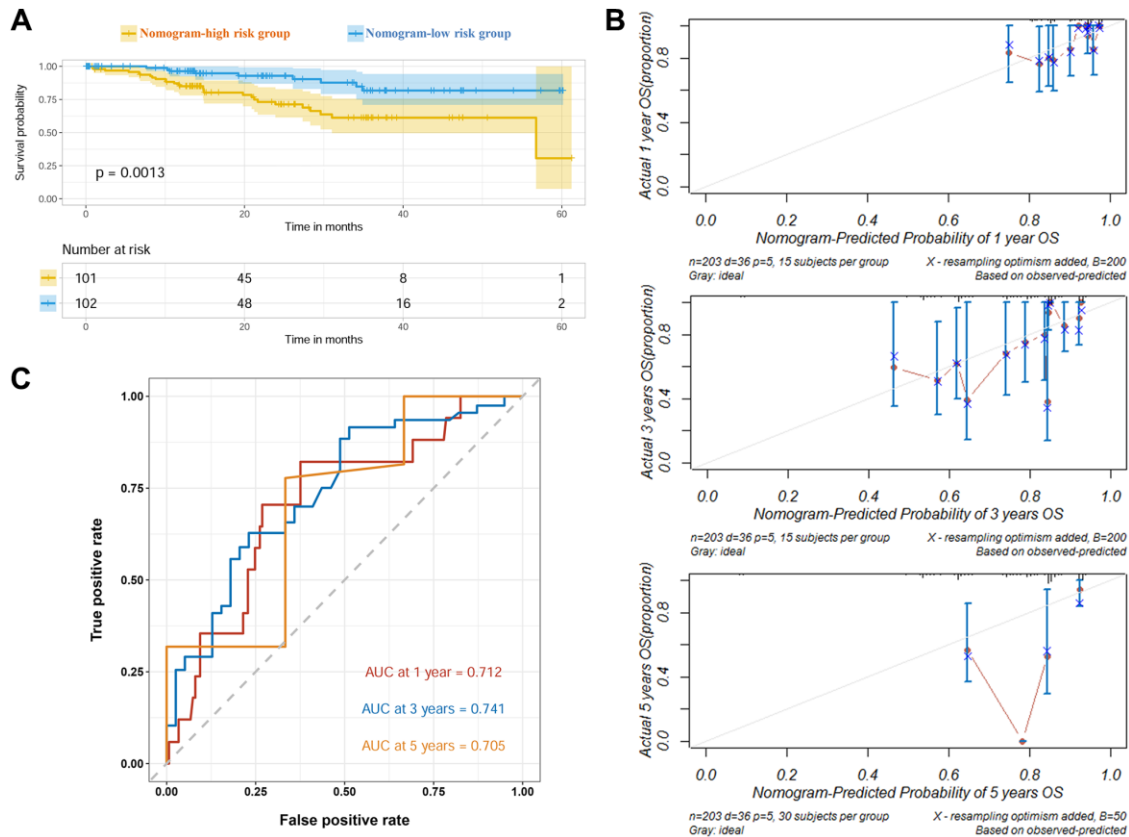


Figure 4. Verification of the prognostic nomogram in CPTAC cohort. (A) Survival curves of high and low nomogram risk groups plotted by K-M method. **(B)** Calibration curves of the nomogram at 1, 3 and 5 years. **(C)** ROC curves of the nomogram at 1, 3 and 5 years.

account for a quarter of all subtypes in high TRG risk group and outnumbered the lower risk group. C6 was found to display the highest TGF- β signature and a high lymphocytic infiltration with an even amount of type I and type II T cells [21]. As compared with other subtypes, C6 specifically showed an enrichment in *KRAS* G12 mutations. C6 subtype was reported to confer the worst favorable outcome in its constituent tumors, and showed complex features reflecting a macrophage dominated, low lymphocyte infiltration, with high M2/M1 macrophage ratio, consistent with an

immunosuppressed tumor microenvironment for which a poor outcome would be expected [21]. The immune subtype analysis indicated that the poor prognosis of patients in the TRG high risk group might be due to the higher portion of C6 subtype.

A higher TMB in tumor is usually considered as a biomarker to estimate the potential benefit of immune checkpoint blockade therapy. Our study showed that the TRG high risk group in LUAD was associated with a significantly higher TMB. Besides, the TRG high risk

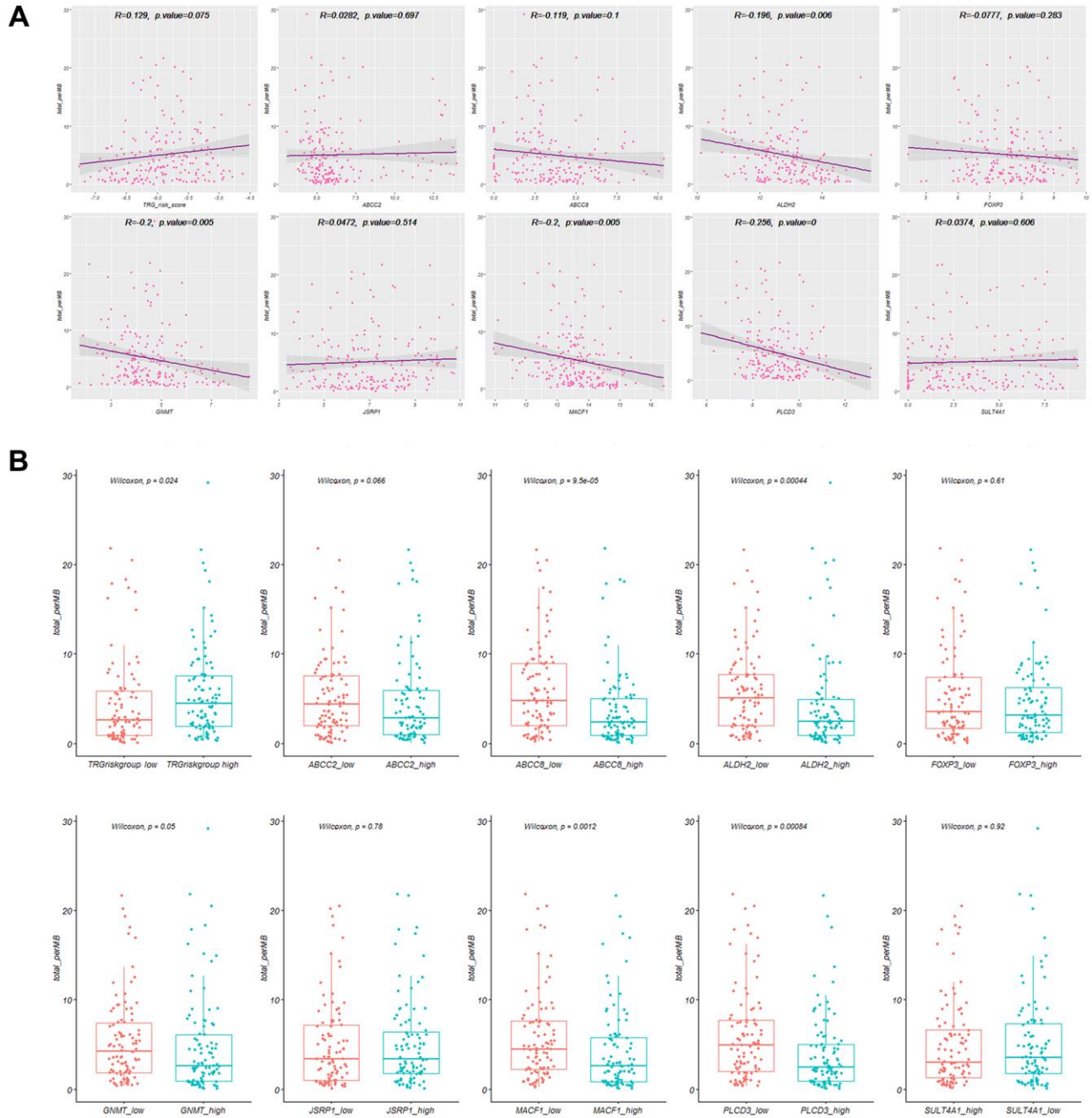


Figure 5. Tumor mutation burden (TMB) correlation with TRGs. (A) The correlation plots of TMB with TRG risk score and nine hub TRGs. **(B)** Level of TMB in high and low TRG risk score groups and nine hub TRGs expression.

group harbored a lower TIDE score indicating that these patients might have relatively better response to immunotherapy. The drug sensitivity estimation analysis results suggested that the high-risk group patients might be more sensitive to Bortezomib, Docetaxel and Staurosporine. On the other hand, patients in the TRG low risk group might benefit from Eg5 treatment. In brief, the patients with a high TRG risk score might be more suitable candidates to receive immune checkpoint inhibitors and had less limited selection of treatment.

The genes in the TRG risk score have been reported to play multiple roles in disease especially cancers. ABCC2 is a multidrug resistance-associated protein in cancer and associated with resistance to cisplatin. The

knockdown ABCC2 could reverse cisplatin resistance in lung cancer cells [26]. And ABCC8 is closely related to immune infiltration of macrophages M2. Studies have shown that knocking out ABCC8 in mice can reduce the infiltration of pro-inflammatory macrophages [27], while promoting the macrophage M2 phenotype (CD163) over the M1 phenotype (CD86) [28]. ALDH2 polymorphisms is found to be related to cancer occurrence and development. Besides, ALDH2 is a biomarker of cancer stem cells (CSCs) and is associated with proliferation, invasiveness, and multidrug resistance to chemotherapy reagents [29]. Recently, the MACF1 mutation was found to be a potential prognostic biomarker and therapeutic target for breast cancer. Patients with MACF1 mutation harbored a poor prognosis and higher tumor mutation burden score.

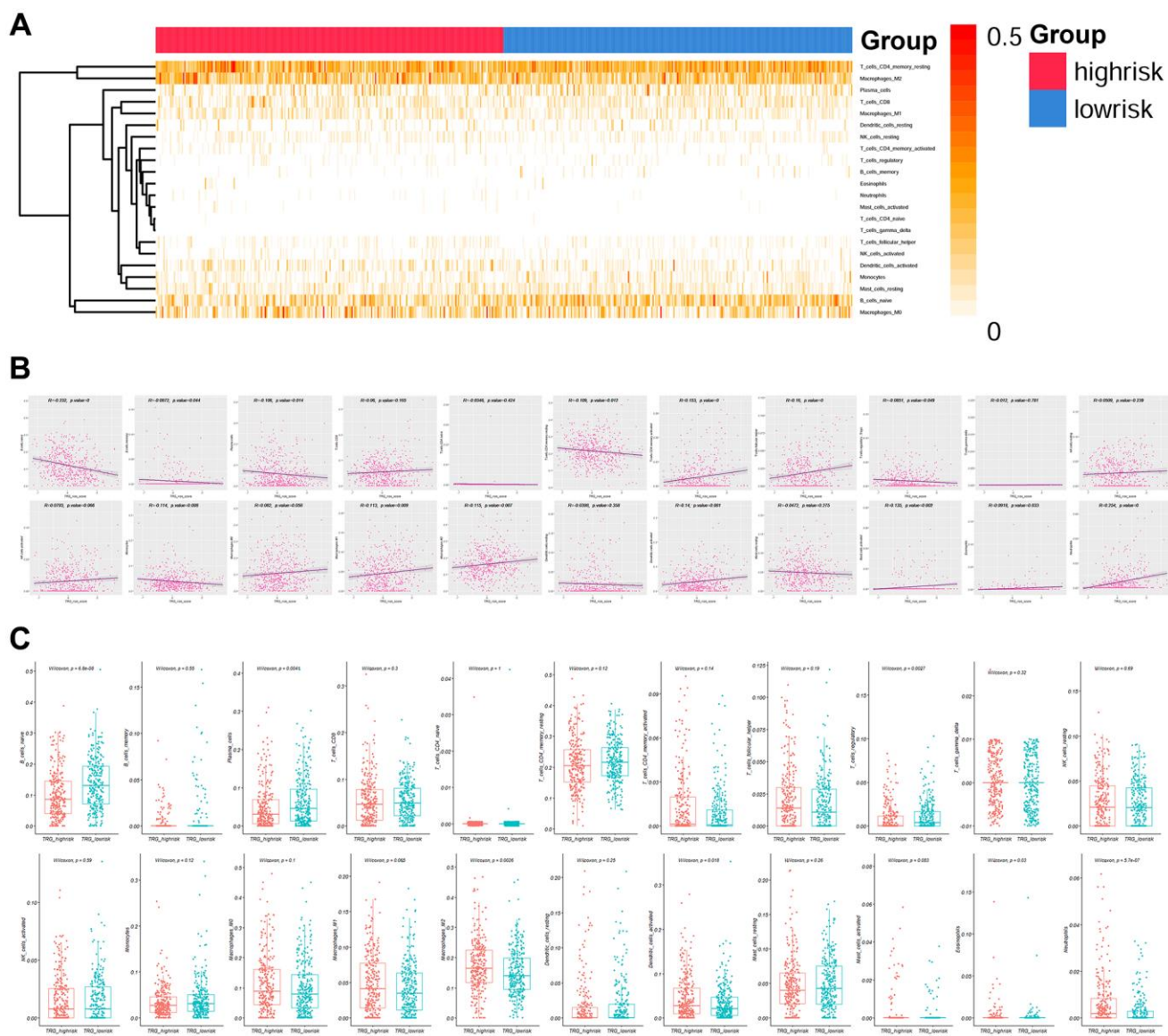


Figure 6. Immune infiltration analysis. (A) Heatmap showing the infiltration percentage of 22 types of immune cells in high and low TRG risk score groups. (B) and (C) Correlation of the infiltration percentage of 22 types of immune cells with TRG risk score.

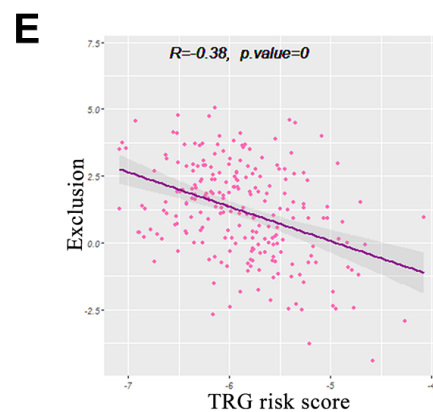
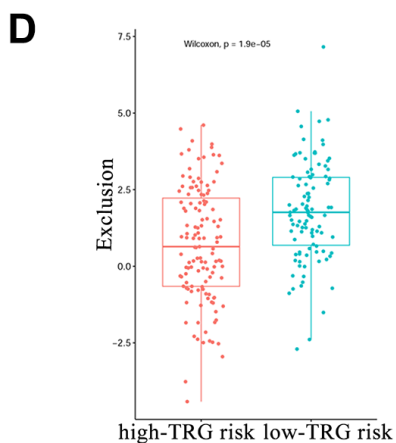
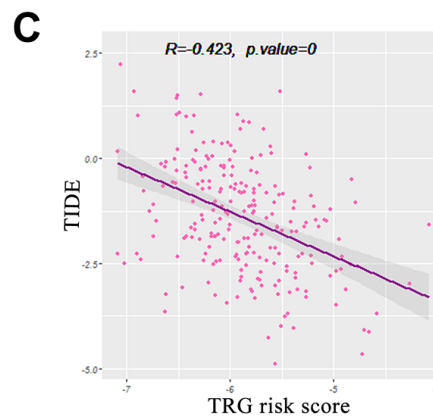
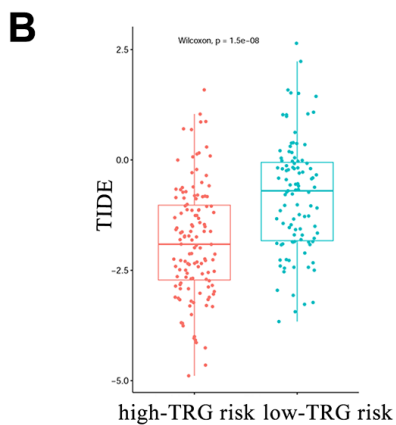
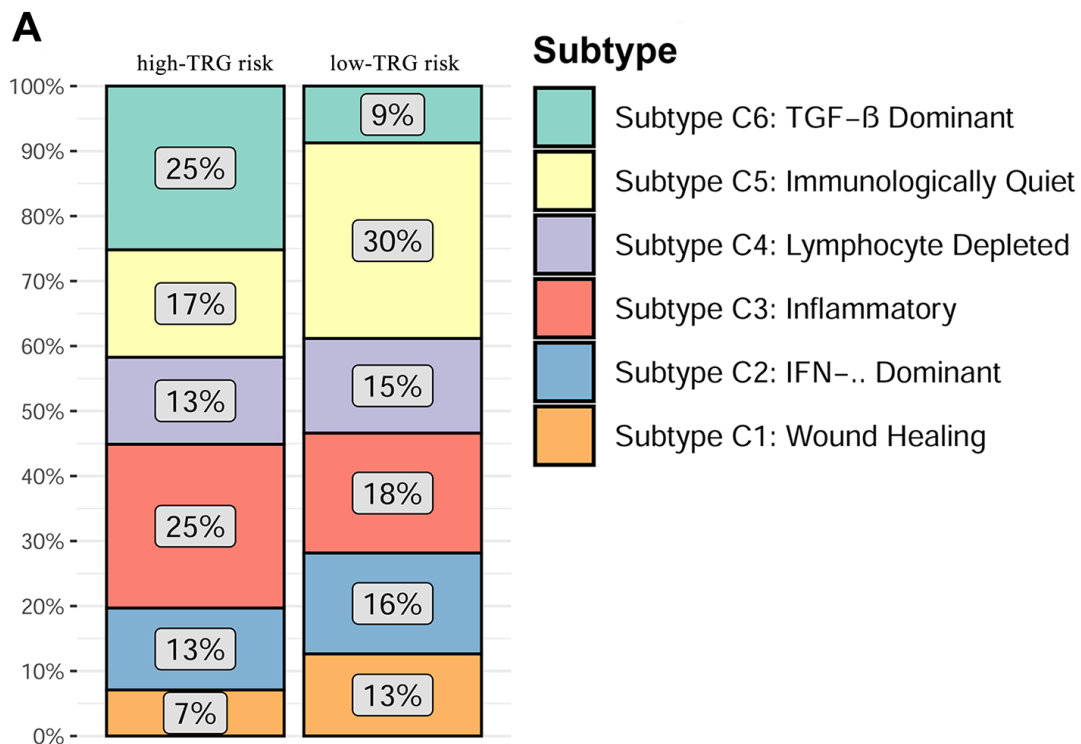


Figure 7. Immune subtypes of the TRGs risk group. (A) Percentage of the six immune subtypes in the high and low TRGs risk groups. (B) and (C) Correlation of the TIDE score with TRG risk score. (D) and (E) Correlation of the exclusion score with TRG risk score.

MACF1 mutation was also found to upregulate the mTOR signaling pathway and change tumor immune microenvironment [30]. In a word, the hubTRGs can participate in the tumorigenesis, cancer cell proliferation and metastasis in various pathways.

This study has several limitations. Firstly, despite that we used a large TCGA database to construct the prognostic model and another database for external

validation, we cannot perform an independent clinical trial to verify these findings due to the long duration of translation and follow-up and the high cost. Secondly, since the analysis in this study was performed by using transcriptomics data, which might limit the clinical promotion of the TRGs risk model, and a further simple and convenient method should be developed. Thirdly, we were unable to verify these findings under different genetic backgrounds due to the lack of racial data,

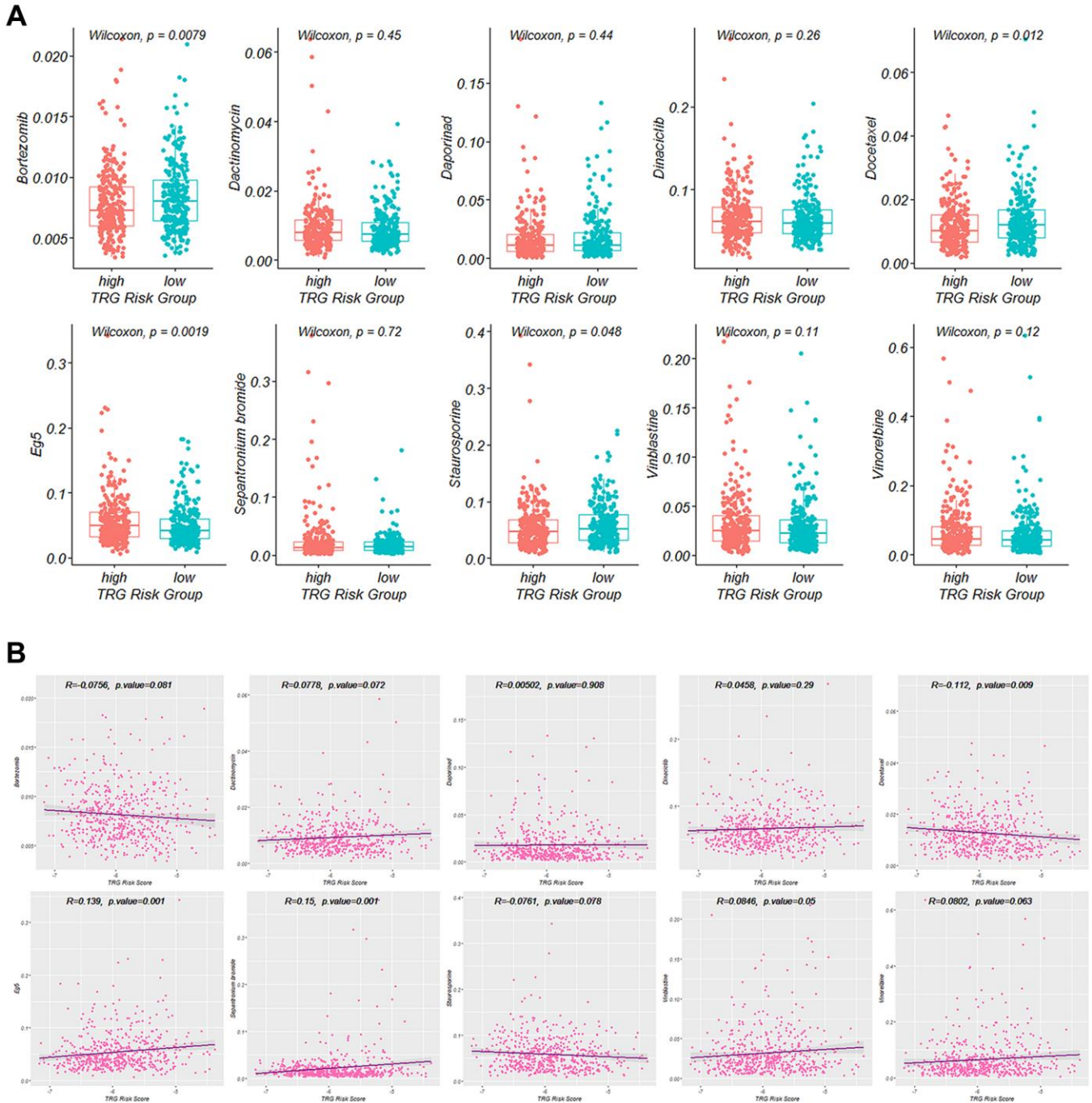


Figure 8. Targeted agents' treatment sensitivity. (A) and (B) Correlation of the IC50 value of the selected ten drugs with TRG risk score.

which requires further research in the future. Lastly, more basic experiments are needed to further clarify the functions and mechanisms of the 9 hubTRGs in LUAD.

CONCLUSION

In this study, we have constructed and validated a risk model based on telomere-related genes in lung adenocarcinoma using the two databases. The TRG signature we have identified might be of help in the selection of treatment reagents for lung adenocarcinoma patients.

AUTHOR CONTRIBUTIONS

(I) Conception and design: HC, YL and XP. (II) Administrative support: WL and XP. (III) Provision of study materials or patients: WZ, FL and YL. (IV) Collection and assembly of data: HC, WL, WZ and FL. (V) Data analysis and interpretation: HC, WL and WZ. (VI) Manuscript writing: All authors. (VII) Final approval of manuscript: All authors.

CONFLICTS OF INTEREST

The authors declare no conflicts of interest related to this study.

FUNDING

This work was supported by the Funds of Medical Science and Technology Innovation Platform Construction Project belonged to the sub-item of Foshan Science and Technology Innovation Project under Contract No. (FSOAA-KJ218-1301-0036 and FSOAA-KJ218-1301-0037).

REFERENCES

1. Sung H, Ferlay J, Siegel RL, Laversanne M, Soerjomataram I, Jemal A, Bray F. Global Cancer Statistics 2020: GLOBOCAN Estimates of Incidence and Mortality Worldwide for 36 Cancers in 185 Countries. *CA Cancer J Clin.* 2021; 71:209–49. <https://doi.org/10.3322/caac.21660> PMID:[33538338](https://pubmed.ncbi.nlm.nih.gov/33538338/)
2. Bray F, Ferlay J, Soerjomataram I, Siegel RL, Torre LA, Jemal A. Global cancer statistics 2018: GLOBOCAN estimates of incidence and mortality worldwide for 36 cancers in 185 countries. *CA Cancer J Clin.* 2018; 68:394–424. <https://doi.org/10.3322/caac.21492> PMID:[30207593](https://pubmed.ncbi.nlm.nih.gov/30207593/)
3. Li Y, Xu C, Yu Q. Risk factor analysis of bone metastasis in patients with non-small cell lung cancer. *Am J Transl Res.* 2022; 14:6696–702. PMID:[36247263](https://pubmed.ncbi.nlm.nih.gov/36247263/)
4. Wang CX, Xu C, Li C, Ding C, Chen J, Zhao J. Significance of risk factor analysis and dissection for station 4L lymphatic metastasis in left lung cancer: a systematic review and meta-analysis. *Transl Cancer Res.* 2021; 10:1656–66. <https://doi.org/10.21037/tcr-20-3339> PMID:[35116491](https://pubmed.ncbi.nlm.nih.gov/35116491/)
5. Zhou E, Wu F, Guo M, Yin Z, Li Y, Li M, Xia H, Deng J, Yang G, Jin Y. Identification of a novel gene signature of lung adenocarcinoma based on epidermal growth factor receptor-tyrosine kinase inhibitor resistance. *Front Oncol.* 2022; 12:1008283. <https://doi.org/10.3389/fonc.2022.1008283> PMID:[36530971](https://pubmed.ncbi.nlm.nih.gov/36530971/)
6. Zeng Z, Liang Y, Shi J, Xiao L, Tang L, Guo Y, Chen F, Lin G. Identification and Application of a Novel Immune-Related lncRNA Signature on the Prognosis and Immunotherapy for Lung Adenocarcinoma. *Diagnostics (Basel).* 2022; 12:2891. <https://doi.org/10.3390/diagnostics12112891> PMID:[36428951](https://pubmed.ncbi.nlm.nih.gov/36428951/)
7. Chen Y, Tang L, Huang W, Zhang Y, Abisola FH, Li L. Identification and validation of a novel cuproptosis-related signature as a prognostic model for lung adenocarcinoma. *Front Endocrinol (Lausanne).* 2022; 13:963220. <https://doi.org/10.3389/fendo.2022.963220> PMID:[36353226](https://pubmed.ncbi.nlm.nih.gov/36353226/)
8. Arimura-Omori M, Kiyohara C, Yanagihara T, Yamamoto Y, Ogata-Suetsugu S, Harada E, Hamada N, Tsuda T, Takata S, Shimabukuro I, Nagata N, Yatera K, Torii R, et al. Association between Telomere-Related Polymorphisms and the Risk of IPF and COPD as a Precursor Lesion of Lung Cancer: Findings from the Fukuoka Tobacco-Related Lung Disease (FOLD) Registry. *Asian Pac J Cancer Prev.* 2020; 21:667–73. <https://doi.org/10.31557/APJCP.2020.21.3.667> PMID:[32212792](https://pubmed.ncbi.nlm.nih.gov/32212792/)
9. Shay JW, Wright WE. Telomeres and telomerase: three decades of progress. *Nat Rev Genet.* 2019; 20:299–309. <https://doi.org/10.1038/s41576-019-0099-1> PMID:[30760854](https://pubmed.ncbi.nlm.nih.gov/30760854/)
10. Savage SA. Beginning at the ends: telomeres and human disease. *F1000Res.* 2018; 7:F1000. <https://doi.org/10.12688/f1000research.14068.1> PMID:[29770205](https://pubmed.ncbi.nlm.nih.gov/29770205/)

11. Lee OH, Kim H, He Q, Baek HJ, Yang D, Chen LY, Liang J, Chae HK, Safari A, Liu D, Songyang Z. Genome-wide YFP fluorescence complementation screen identifies new regulators for telomere signaling in human cells. *Mol Cell Proteomics*. 2011; 10:M110.001628. <https://doi.org/10.1074/mcp.M110.001628> PMID:21044950
12. Shay JW. Role of Telomeres and Telomerase in Aging and Cancer. *Cancer Discov*. 2016; 6:584–93. <https://doi.org/10.1158/2159-8290.CD-16-0062> PMID:27029895
13. Lin X, Gu J, Lu C, Spitz MR, Wu X. Expression of telomere-associated genes as prognostic markers for overall survival in patients with non-small cell lung cancer. *Clin Cancer Res*. 2006; 12:5720–5. <https://doi.org/10.1158/1078-0432.CCR-05-2809> PMID:17020976
14. Kim S, Chowdhury T, Yu HJ, Kahng JY, Lee CE, Choi SA, Kim KM, Kang H, Lee JH, Lee ST, Won JK, Kim KH, Kim MS, et al. The telomere maintenance mechanism spectrum and its dynamics in gliomas. *Genome Med*. 2022; 14:88. <https://doi.org/10.1186/s13073-022-01095-x> PMID:35953846
15. Sung JY, Cheong JH. Pan-Cancer Analysis of Clinical Relevance via Telomere Maintenance Mechanism. *Int J Mol Sci*. 2021; 22:11101. <https://doi.org/10.3390/ijms22011101> PMID:34681758
16. Li SC, Jia ZK, Yang JJ, Ning XH. Telomere-related gene risk model for prognosis and drug treatment efficiency prediction in kidney cancer. *Front Immunol*. 2022; 13:975057. <https://doi.org/10.3389/fimmu.2022.975057> PMID:36189312
17. Liu XG, Li M, Mai SJ, Cai RJ. Telomere length-related signature as a novel biomarker of prognosis and immune response in non-small cell lung cancer. *Eur Rev Med Pharmacol Sci*. 2022; 26:1304–19. https://doi.org/10.26355/eurrev_202202_28124 PMID:35253187
18. Braun DM, Chung I, Kepper N, Deeg KI, Rippe K. TelNet - a database for human and yeast genes involved in telomere maintenance. *BMC Genet*. 2018; 19:32. <https://doi.org/10.1186/s12863-018-0617-8> PMID:29776332
19. Newman AM, Liu CL, Green MR, Gentles AJ, Feng W, Xu Y, Hoang CD, Diehn M, Alizadeh AA. Robust enumeration of cell subsets from tissue expression profiles. *Nat Methods*. 2015; 12:453–7. <https://doi.org/10.1038/nmeth.3337> PMID:25822800
20. Maeser D, Gruener RF, Huang RS. oncoPredict: an R package for predicting in vivo or cancer patient drug response and biomarkers from cell line screening data. *Brief Bioinform*. 2021; 22:bbab260. <https://doi.org/10.1093/bib/bbab260> PMID:34260682
21. Thorsson V, Gibbs DL, Brown SD, Wolf D, Bortone DS, Ou Yang TH, Porta-Pardo E, Gao GF, Plaisier CL, Eddy JA, Ziv E, Culhane AC, Paull EO, et al. The Immune Landscape of Cancer. *Immunity*. 2018; 48:812–30.e14. <https://doi.org/10.1016/j.immuni.2018.03.023> PMID:29628290
22. Cao X, Huang M, Zhu M, Fang R, Ma Z, Jiang T, Dai J, Ma H, Jin G, Shen H, Du J, Xu L, Hu Z. Mendelian randomization study of telomere length and lung cancer risk in East Asian population. *Cancer Med*. 2019; 8:7469–76. <https://doi.org/10.1002/cam4.2590> PMID:31605466
23. Xue Y, Guo X, Huang X, Zhu Z, Chen M, Chu J, Yang G, Wang Q, Kong X. Shortened telomere length in peripheral blood leukocytes of patients with lung cancer, chronic obstructive pulmonary disease in a high indoor air pollution region in China. *Mutat Res Genet Toxicol Environ Mutagen*. 2020; 858–860:503250. <https://doi.org/10.1016/j.mrgentox.2020.503250> PMID:33198931
24. Alder JK, Armanios M. Telomere-mediated lung disease. *Physiol Rev*. 2022; 102:1703–20. <https://doi.org/10.1152/physrev.00046.2021> PMID:35532056
25. Siwik CJ, Cash E, Sephton SE. Depressive symptoms and shorter survival in lung cancer: the role of leukocyte telomere length. *Psychol Health*. 2022. [Epub ahead of print]. <https://doi.org/10.1080/08870446.2022.2040500> PMID:35240880
26. Chen Y, Zhou H, Yang S, Su D. Increased ABCC2 expression predicts cisplatin resistance in non-small cell lung cancer. *Cell Biochem Funct*. 2021; 39:277–86. <https://doi.org/10.1002/cbf.3577> PMID:32815556
27. Makar TK, Gerzanich V, Nimmagadda VK, Jain R, Lam K, Mubariz F, Trisler D, Ivanova S, Woo SK, Kwon MS, Bryan J, Bever CT, Simard JM. Silencing of Abcc8 or inhibition of newly upregulated Sur1-Trpm4 reduce inflammation and disease progression in experimental autoimmune encephalomyelitis. *J Neuroinflammation*. 2015; 12:210. <https://doi.org/10.1186/s12974-015-0432-3> PMID:26581714

28. Gerzanich V, Makar TK, Guda PR, Kwon MS, Stokum JA, Woo SK, Ivanova S, Ivanov A, Mehta RI, Morris AB, Bryan J, Bever CT, Simard JM. Salutory effects of glibenclamide during the chronic phase of murine experimental autoimmune encephalomyelitis. *J Neuroinflammation*. 2017; 14:177.
<https://doi.org/10.1186/s12974-017-0953-z>
PMID:[28865458](https://pubmed.ncbi.nlm.nih.gov/28865458/)
29. Kallifatidis G, Smith DK, Morera DS, Gao J, Hennig MJ, Hoy JJ, Pearce RF, Dabke IR, Li J, Merseburger AS, Kuczyk MA, Lokeshwar VB, Lokeshwar BL. β -Arrestins Regulate Stem Cell-Like Phenotype and Response to Chemotherapy in Bladder Cancer. *Mol Cancer Ther*. 2019; 18:801–11.
<https://doi.org/10.1158/1535-7163.MCT-18-1167>
PMID:[30787175](https://pubmed.ncbi.nlm.nih.gov/30787175/)
30. Tian Y, Zhu K, Li Y, Ren Z, Wang J. MACF1 mutations predict poor prognosis: a novel potential therapeutic target for breast cancer. *Am J Transl Res*. 2022; 14:7670–88.
PMID:[36505342](https://pubmed.ncbi.nlm.nih.gov/36505342/)

SUPPLEMENTARY MATERIALS

Supplementary Tables

Supplementary Table 1. Differentially expressed telomere-related gene in LUAD.

TRG	logFC	P value	TRG	logFC	P value	TRG	logFC	P value	TRG	logFC	P value
ANGPT4	-4.85	5.03E-84	KLF2	-2.13	8.47E-37	TDRD10	-1.58	6.32E-09	JUNB	-1.18	1.33E-18
TNNC1	-4.5	3.40E-59	GATA2	-2.11	5.10E-38	AR	-1.58	9.09E-13	CSRP1	-1.18	2.97E-42
ANXA8L1	-4.49	1.01E-41	ALDH1A1	-2.09	1.12E-18	USP2	-1.58	6.29E-17	MYO1C	-1.18	4.83E-38
SH3GL2	-4.47	3.47E-47	PRKCQ	-2.09	4.06E-34	DYDC1	-1.57	5.96E-14	MACF1	-1.16	6.75E-17
GPA33	-4.24	1.66E-52	LGALS1	-2.09	1.32E-44	PHYHD1	-1.56	2.66E-11	TXNIP	-1.16	2.84E-14
FHL1	-4.08	8.23E-76	PLCL1	-2.08	1.57E-50	ELOVL3	-1.56	2.94E-10	ABCC6	-1.16	3.18E-10
FOSB	-3.88	2.17E-29	PNMT	-2.08	3.09E-14	SYNE1	-1.52	9.90E-18	SYDE1	-1.15	1.88E-22
PTPN5	-3.75	1.21E-62	DAW1	-2.05	5.00E-13	CEBPA	-1.51	3.69E-14	EPHX2	-1.15	6.48E-13
PRX	-3.63	9.87E-76	ABCC8	-2.02	1.56E-10	DST	-1.5	1.40E-15	FOXO1	-1.15	3.96E-19
XAGE2	-3.55	1.49E-19	SULT1B1	-2.01	9.92E-19	ABCC9	-1.5	3.51E-18	SMARCA2	-1.14	4.56E-24
ZBTB16	-3.48	5.48E-27	LRCH2	-2	4.94E-25	MITF	-1.5	6.03E-29	TNIP3	-1.13	2.64E-06
PCSK9	-3.34	5.70E-23	WFS1	-1.97	4.31E-55	ARRDC4	-1.48	3.63E-26	PLCD3	-1.13	3.65E-11
ANOS1	-3.34	5.83E-55	PDE1B	-1.97	5.25E-42	DMD	-1.44	7.69E-17	RAPGEF3	-1.13	4.80E-15
FGFR4	-3.32	3.53E-40	KLF6	-1.97	1.16E-52	SYDE2	-1.42	1.10E-18	FOXO4	-1.12	1.73E-29
LRRC18	-3.28	3.47E-32	EGR1	-1.96	9.33E-23	LRRC25	-1.41	1.48E-20	TNIK	-1.12	8.90E-10
IQSEC3	-3.17	4.21E-57	PPP1R17	-1.94	5.38E-27	HOXA7	-1.4	3.25E-14	LRCH1	-1.1	3.99E-31
TAL1	-3.08	5.44E-79	AHNAK	-1.92	2.98E-27	PRKD1	-1.4	2.74E-19	BIN2	-1.1	3.89E-16
TUBB1	-3.07	4.82E-59	FLII	-1.91	5.53E-50	VAMP2	-1.39	7.02E-38	ITGAX	-1.1	8.85E-13
WDR38	-3	1.96E-16	S100A8	-1.9	4.01E-13	ETS1	-1.39	8.29E-27	MSN	-1.09	2.19E-20
PDK4	-2.91	6.85E-38	FBP1	-1.89	2.95E-31	PPM1F	-1.38	5.01E-56	NR2F1	-1.09	3.81E-13
CLIC3	-2.84	1.83E-27	CDK15	-1.87	2.10E-22	RARRES2	-1.38	3.72E-16	NEK7	-1.09	1.01E-30
MYOCD	-2.81	5.94E-27	NLGN4X	-1.86	2.34E-15	TFRC	-1.38	2.93E-21	SLC7A8	-1.07	9.03E-09
KLF4	-2.7	1.44E-42	PRDM16	-1.86	3.60E-11	KAT2B	-1.38	1.73E-32	PRKCB	-1.07	1.57E-11
SNX22	-2.63	1.24E-54	ZFP42	-1.82	1.50E-05	NCBP2L	-1.36	3.87E-13	PAPSS1	-1.07	2.58E-51
CFTR	-2.57	8.81E-15	ADPRH	-1.8	1.32E-61	FGFR3	-1.36	8.27E-07	TLN1	-1.07	1.04E-28
ASPG	-2.57	4.72E-15	CDKN2B	-1.8	2.27E-22	ARHGAP23	-1.35	2.04E-24	OSBPL11	-1.06	9.54E-51
EPAS1	-2.54	1.74E-75	KLF9	-1.79	9.71E-41	TFEC	-1.34	3.79E-14	FOXN3	-1.06	1.89E-25
ALPL	-2.5	3.00E-17	FOS	-1.79	9.86E-18	CHD5	-1.34	4.18E-12	HHATL	-1.06	0.001297
MACROD2	-2.43	3.60E-17	FOXF2	-1.76	1.08E-23	PALM	-1.33	4.47E-17	PLCL2	-1.05	1.88E-15
CFAP58	-2.41	8.33E-27	TCEAL7	-1.75	1.23E-32	LRRC63	-1.29	4.08E-13	ARHGAP20	-1.05	2.34E-06
KCTD16	-2.37	3.92E-33	MYH10	-1.73	3.90E-37	PTPRG	-1.29	6.74E-19	MECOM	-1.05	1.12E-08
PAK5	-2.35	5.93E-25	SLC7A7	-1.73	2.16E-35	THEMIS2	-1.28	1.89E-25	JAK2	-1.04	6.56E-19
GATA6	-2.33	2.44E-36	ETV1	-1.73	2.90E-21	FERMT3	-1.28	1.19E-18	BMP7	-1.04	0.0004118
SOX5	-2.31	9.75E-38	TDRD9	-1.72	4.36E-11	JUN	-1.27	2.13E-20	JAZF1	-1.04	2.08E-21
GATA5	-2.3	1.67E-25	RYR2	-1.72	1.72E-15	IRS4	-1.27	7.17E-09	CREB5	-1.02	1.26E-08
SIRPD	-2.28	3.86E-40	ZEB2	-1.7	2.96E-30	IP6K3	-1.26	0.0001382	TRIM22	-1.02	1.54E-12
KLF17	-2.27	1.97E-36	PLCB4	-1.69	5.54E-12	ARL11	-1.26	8.13E-18	MT1X	-1.01	1.76E-07
DOK2	-2.24	2.48E-39	PLCE1	-1.68	1.12E-30	DOCK2	-1.25	5.16E-16	ARHGAP28	-1	3.55E-08
PDLIM2	-2.23	3.11E-67	ARRB1	-1.67	8.46E-38	NEATC1	-1.24	2.24E-24	BAIAP2L1	1	4.61E-23
DYDC2	-2.22	6.85E-14	AK1	-1.66	4.66E-24	GABRB3	-1.23	0.0007302	BASP1	1.01	1.67E-07
KLF15	-2.22	2.31E-21	TUBB6	-1.66	2.60E-33	CDK14	-1.22	1.01E-17	GMNN	1.01	3.55E-21
GATA1	-2.22	4.06E-36	SLC6A12	-1.65	3.53E-20	MAP3K3	-1.21	2.95E-41	GLDC	1.01	0.0001704
CAMK2A	-2.21	7.08E-41	GNMT	-1.61	7.52E-19	ETS2	-1.2	1.70E-21	PKIB	1.02	7.91E-06
PPARG	-2.18	6.40E-25	UTRN	-1.61	5.33E-32	GATA3	-1.19	1.79E-13	LRRIQ4	1.02	2.56E-05
TBX2	-2.16	1.27E-42	JUND	-1.6	3.43E-36	ANXA1	-1.19	2.22E-09	POC1A	1.02	2.68E-17
MYOM2	-2.15	5.04E-30	ALDH2	-1.59	1.19E-27	CDKL2	-1.19	7.44E-07	CHEK2	1.02	1.07E-20
DSG2	1.02	5.57E-12	PC	1.4	5.39E-26	RMI2	1.87	1.37E-48	IGF2BP1	2.8	1.94E-09
TFAP4	1.03	1.74E-32	MCM2	1.4	4.05E-21	ASF1B	1.89	1.25E-37	CENPF	2.82	4.70E-51
GAP43	1.03	0.0001926	EDN2	1.41	5.29E-06	CHEK1	1.9	1.61E-35	HMGB3	2.84	6.90E-43
DSCC1	1.04	9.30E-13	CHAF1B	1.42	1.12E-36	PACSIN1	1.92	4.90E-20	EXO1	2.86	7.46E-48

ZC3HAV1L	1.05	2.30E-17	RAD54B	1.42	7.61E-26	TDRD5	1.94	8.78E-07	AURKB	2.89	9.61E-46
ATAD5	1.05	2.24E-18	RHPN1	1.44	5.16E-16	AURKA	1.96	2.31E-33	HMGA2	2.97	2.49E-10
GMDS	1.06	4.98E-19	ATAD2	1.45	1.02E-28	ABCY6	1.97	3.49E-31	AKR7A3	2.99	3.42E-17
TTBK1	1.07	1.14E-11	FANCI	1.47	5.84E-34	RHBDL2	1.98	1.41E-29	PCP4	3.05	2.39E-12
RACGAP1	1.07	6.76E-18	CALML6	1.47	2.81E-11	SLC7A11	1.99	1.84E-12	NEK2	3.09	1.17E-52
TDRKH	1.08	1.35E-24	KAT2A	1.48	7.00E-40	BRIP1	2	4.49E-36	CDC20	3.13	1.25E-52
S100A7	1.09	0.0031685	FOXP3	1.49	1.47E-22	EZH2	2.04	5.04E-52	TFAP2A	3.14	2.75E-33
HRG	1.11	5.69E-07	FANCA	1.51	3.76E-36	TRIP13	2.05	3.81E-28	ETV4	3.17	3.14E-53
NME4	1.11	1.48E-19	RCC1	1.51	7.06E-54	CLSPN	2.05	4.51E-35	KIF4A	3.18	1.38E-56
SLC7A9	1.11	2.19E-05	BLM	1.51	1.45E-30	ABCC3	2.07	7.32E-24	TOP2A	3.32	8.46E-63
CCT3	1.11	5.80E-39	ARL14	1.52	9.51E-05	ORC1	2.08	4.67E-35	TUBB3	3.56	2.29E-53
RNF222	1.12	5.33E-07	AVPR1B	1.53	5.07E-09	JSRP1	2.09	6.70E-15	TERT	3.66	3.62E-40
LDHA	1.12	7.61E-33	HGD	1.53	3.51E-05	EME1	2.1	1.89E-36	AKR1B10	3.7	9.98E-11
PRDX4	1.15	3.28E-23	RAD51	1.53	6.05E-25	SLC7A5	2.11	1.22E-28	PITX1	4	1.71E-28
CCNE2	1.15	1.06E-14	PNCK	1.54	5.58E-08	RHBDL1	2.21	1.79E-21	GREM1	4.03	6.81E-36
FANCD2	1.16	3.16E-32	MYCN	1.55	1.04E-06	CCNA2	2.25	4.07E-39			
ABCC2	1.18	0.0009098	IVL	1.55	0.0019983	COCH	2.27	2.45E-16			
MCM6	1.18	9.63E-28	DBNDD1	1.57	1.33E-27	SLC7A10	2.28	3.16E-09			
E2F3	1.18	5.32E-41	LMNB1	1.57	8.93E-37	RECQL4	2.28	1.34E-42			
RUNX2	1.18	2.67E-18	NAT16	1.57	1.75E-11	IGF2BP3	2.36	3.69E-11			
FOXO6	1.19	8.36E-07	ABCC11	1.58	6.70E-16	HMMR	2.36	3.07E-41			
DNMT3B	1.2	5.93E-15	FOXH1	1.6	4.03E-11	CCNB1	2.37	5.42E-47			
UGDH	1.2	2.46E-13	TUBB8	1.6	3.19E-16	MAST1	2.39	9.51E-32			
FANCB	1.21	6.00E-16	PAICS	1.61	3.36E-60	CDCA8	2.4	3.93E-49			
MAGEA4	1.23	0.0076762	DQX1	1.62	3.15E-09	PKMYT1	2.41	3.40E-39			
FEN1	1.25	2.41E-30	DNA2	1.62	1.61E-32	CCNE1	2.42	1.05E-36			
WDHD1	1.26	5.79E-24	PIF1	1.63	4.00E-22	NDC80	2.43	6.48E-42			
MSH5	1.28	6.19E-14	KPNA2	1.64	5.82E-34	RAD54L	2.48	5.27E-43			
CHTF18	1.3	9.10E-20	POLE2	1.64	9.46E-30	ORC6	2.49	2.23E-54			
PLOD2	1.31	1.23E-11	PFKP	1.66	1.08E-24	NCAPG	2.51	1.38E-39			
RFC4	1.31	5.00E-29	UCHL1	1.66	9.45E-07	XRCC2	2.55	1.26E-48			
CALML5	1.31	0.0007595	TUBB2B	1.66	5.35E-07	PLK1	2.56	2.38E-54			
TXNDC17	1.32	2.02E-22	SULT4A1	1.67	8.92E-06	CDC45	2.57	6.69E-44			
GAPDH	1.33	1.06E-29	ECT2	1.71	2.78E-35	FOXM1	2.6	5.06E-43			
PDK1	1.35	2.16E-27	CDC25A	1.72	7.72E-26	S100P	2.61	7.35E-09			
FANCG	1.35	8.06E-24	PAFAH1B3	1.75	1.31E-29	TBX15	2.61	6.56E-19			
RAD51AP1	1.35	1.69E-18	HMGA1	1.81	5.50E-32	MKI67	2.62	5.63E-46			
RASGEF1C	1.35	2.24E-06	MCM4	1.82	2.48E-42	PSAT1	2.68	3.60E-38			
PAX5	1.36	3.93E-07	E2F2	1.84	9.29E-35	SGO1	2.68	3.06E-44			
RPS10	1.38	1.15E-20	CDK1	1.86	1.66E-30	TRIM15	2.71	3.10E-12			

Abbreviations: TRG: telomere-related gene; LUAD: lung adenocarcinoma.

Supplementary Table 2. Significant TRGs in K-M curve and COX regression analysis.

Similar TRG in K-M	P value	Similar TRG in COX	Hazard ratio	P value	Different TRG in K-M	P value	Different TRG in COX	Hazard ratio	P value
ABCC2	0.007	ABCC2	1.1	0	ADPRH	0.018	ANOS1	0.87	0.002
ABCC6	0.017	ABCC6	0.86	0.005	ARL11	0.017	ARHGAP20	0.91	0.032
ABCC8	0.03	ABCC8	0.91	0.007	HMGA1	0.013	AURKA	1.17	0.02
ALDH2	0.004	ALDH2	0.8	0.001	JAK2	0.045	BIN2	0.82	0.008
ARL14	0.037	ARL14	1.1	0.001	JAZF1	0.001	BLM	1.22	0.018
ARRB1	0.048	ARRB1	0.77	0	KPNA2	0.036	CDC25A	1.19	0.013
AURKB	0.024	AURKB	1.11	0.047	LDHA	0.03	EPAS1	0.84	0.031
CCNA2	0.001	CCNA2	1.24	0	PDE1B	0.036	ETV1	0.9	0.037
CCNB1	0.01	CCNB1	1.22	0.003	RASGEF1C	0.014	FANCI	1.26	0.01
CDC20	0.022	CDC20	1.13	0.024	SMARCA2	0.019	FOXN3	0.78	0.02
CDK1	0.003	CDK1	1.22	0.002	UTRN	0.043	GATA1	0.89	0.042
CDKL2	0	CDKL2	0.87	0.001	XRCC2	0.022	GATA2	0.87	0.033
CEBPA	0.015	CEBPA	0.9	0.031			HHATL	0.9	0.009
CENPF	0.04	CENPF	1.14	0.02			HOXA7	1.16	0.011
CFTR	0.017	CFTR	0.91	0.002			ITGAX	0.85	0.017
CHEK1	0.003	CHEK1	1.27	0.001			KLF4	1.13	0.024
CLSPN	0.018	CLSPN	1.16	0.024			LMNB1	1.19	0.035
DMD	0.043	DMD	0.87	0.019			MYOM2	0.9	0.046
DOCK2	0.018	DOCK2	0.85	0.009			NLGN4X	1.09	0.048
DOK2	0.005	DOK2	0.88	0.03			PCP4	0.95	0.022
DSG2	0.032	DSG2	1.21	0.011			PCSK9	1.07	0.023
ECT2	0	ECT2	1.27	0.001			PHYHD1	0.91	0.026
EPHX2	0.049	EPHX2	0.88	0.036			PITX1	1.06	0.047
EXO1	0.003	EXO1	1.19	0.001			PKIB	1.11	0.026
FBP1	0.002	FBP1	0.83	0.002			PKMYT1	1.17	0.012
FEN1	0.025	FEN1	1.28	0.013			PLOD2	1.13	0.024
FLI1	0.022	FLI1	0.84	0.031			RAPGEF3	0.87	0.037
FOXM1	0.002	FOXM1	1.2	0.001			RHPN1	0.89	0.032
FOXO4	0.037	FOXO4	0.79	0.022			SGO1	1.16	0.007
FOXO6	0.007	FOXO6	0.91	0.035			SLC7A11	1.08	0.04
FOXP3	0.004	FOXP3	0.82	0.005			SYDE2	0.84	0.008
GAP43	0.02	GAP43	1.1	0.012			TRIM22	0.84	0.008
GNMT	0.005	GNMT	0.82	0.001			TUBB6	1.17	0.038
HMGA2	0.031	HMGA2	1.06	0.005			WDHD1	1.33	0.001
HMMR	0.001	HMMR	1.25	0					
HRG	0.006	HRG	1.11	0.021					
IGF2BP1	0.043	IGF2BP1	1.09	0					
IGF2BP3	0.032	IGF2BP3	1.07	0.016					
JSRP1	0.048	JSRP1	0.92	0.041					
KAT2B	0	KAT2B	0.82	0.012					
KIF4A	0.032	KIF4A	1.16	0.008					
KLF15	0.009	KLF15	0.87	0.002					
MACF1	0.042	MACF1	0.79	0.009					
MAP3K3	0.023	MAP3K3	0.72	0.001					
MECOM	0.03	MECOM	0.88	0.024					

MKI67	0.001	MKI67	1.15	0.011
NCAPG	0.02	NCAPG	1.17	0.005
NDC80	0.021	NDC80	1.19	0.004
NEK2	0.001	NEK2	1.16	0.005
NFATC1	0.002	NFATC1	0.82	0.006
PAX5	0.013	PAX5	0.89	0.005
PDLIM2	0.015	PDLIM2	0.86	0.042
PFKP	0.006	PFKP	1.15	0.03
PLCD3	0.014	PLCD3	1.32	0
PLCL1	0.006	PLCL1	0.87	0.048
PLCL2	0.008	PLCL2	0.81	0.009
PLK1	0.001	PLK1	1.27	0
PRDM16	0	PRDM16	0.9	0.002
PRKCB	0.006	PRKCB	0.82	0.001
RACGAP1	0.018	RACGAP1	1.22	0.017
RAD51	0.023	RAD51	1.24	0.003
S100P	0.038	S100P	1.07	0.007
SLC7A8	0.002	SLC7A8	0.86	0.008
SNX22	0.011	SNX22	0.82	0.001
SULT4A1	0.029	SULT4A1	0.94	0.027
SYNE1	0.004	SYNE1	0.84	0.002
TDRD10	0.005	TDRD10	0.88	0.001
TFAP2A	0.004	TFAP2A	1.11	0.007
TFEC	0.031	TFEC	0.89	0.045
THEMIS2	0.03	THEMIS2	0.8	0.006
TNIK	0.002	TNIK	0.85	0.003
TRIM15	0.014	TRIM15	1.08	0.003
VAMP2	0.021	VAMP2	0.8	0.021
ZEB2	0.001	ZEB2	0.85	0.027

Abbreviation: TRG: telomere-related gene.